104 (2025) 105336

Contents lists available at ScienceDirect

Poultry Science

journal homepage: www.elsevier.com/locate/psj

Full-Length Article

Duck plague virus US3 kinase phosphorylates and induces STING degradation to inhibit innate immune responses

Bin Tian [a,1], Yanming Tian [a,1], Dongjie Cai [a,1], Huanhuan Cao [a], Liping Wu [a], Mingshu Wang [a], Qiao Yang [a], Ying Wu [a], Renyong Jia [a], Dekang Zhu [a], Mafeng Liu [a], Shun Chen [a], Xinxin Zhao [a], Shaqiu Zhang [a], Juan Huang [a], Di Sun [a], Xumin Ou [a], Zhen Wu [a], Anchun Cheng [a,b,*]

[a] Engineering Research Center of Southwest Animal Disease Prevention and Control Technology for Ministry of Education of the People's Republic of China, International Joint Research Center for Animal Disease Prevention and Control of Sichuan Province, Key Laboratory of Animal Disease and Human Health of Sichuan Province, Research Center of Avian Disease and Institute of Veterinary Medicine and Immunology, College of Veterinary Medicine, Sichuan Agricultural University, Chengdu 611130, China

[b] Veterinary Department in College of Aminal Science, State Key Laboratory of Green Pesticide, Institute of Veterinary Immunology and Green Drugs, Guizhou University, Guiyang 550025, China

ARTICLE INFO

Keywords:
Alpha herpesvirus
US3 kinase
STING
Phosphorylation
Immune evasion

ABSTRACT

Duck plague virus (DPV) causes the highest mortality rate among aquatic birds; however, its antago nistic mechanism against antiviral innate immune responses remains elusive. In this study, we systematically screened and found that most DPV genes have inhibitory potential for duck cyclic guanosine monophosphate-adenosine monophosphate synthetase (cGAS)/stimulator of interferon (IFN) gene (STING) pathway-mediated antiviral responses, with the DPV US3 kinase showing the strongest inhibitory activity. Co-immunoprecipitation and immunoblotting assays demonstrated that DPV US3 interacted with STING and induced its degradation. Further mutagenesis experiments revealed that DPV US3 kinase activity was essential for phosphorylating STING, reducing STING dimerization, and inhibiting STING-mediated antiviral responses. Sequence alignment and mutagenesis studies have demonstrated that DPV US3 phosphorylates STING at serine 86, near the Endoplasmic reticulum (ER) retention sequence ($R_{82}YRGS_{86}$), disrupting its association with tank-binding kinase 1 (TBK1) and inducing STING degradation. Finally, US3 knockout attenuated DPV replication by activating higher levels of IFN and ISGs *in vitro* and *in vivo*. These results demonstrate that DPV promotes viral infection and pathogenicity by inducing STING degradation through the encoded US3 kinase, providing new insights into the mechanism of DPV immune evasion.

Introduction

Duck plague virus (DPV) belongs to the Herpesviridae family and Alpha herpesviridae subfamilies (Converse and Kidd, 2001; Roizmann, et al., 1992), causing severe disease in aquatic birds, known as duck plague (DP). DP is an acute or sometimes chronic, highly contagious disease characterized by high morbidity (up to 100%) and mortality rates (up to 95%) among ducks, swans, geese, and other waterfowl, resulting in significant economic losses for the poultry industry (Qi, et al., 2008; Yuan, et al., 2005). The disease has been reported in both domestic and wild waterfowl across various countries, including the Netherlands, the USA, China, France, Belgium, India, Thailand, England, Canada, Hungary, Denmark, Austria, Vietnam, Germany, Bangladesh, Egypt, and Poland (Dhama, et al., 2017). DPV is the only herpesvirus identified in aquatic birds and is associated with the highest mortality rates within the Alpha herpesviridae subfamily. Infection with virulent DPV strains causes systemic lesions in multiple tissues of ducks, including the heart, liver, spleen, bursa, and brain (Chen, et al., 2017; Li,

* Corresponding author at: Engineering Research Center of Southwest Animal Disease Prevention and Control Technology for Ministry of Education of the People's Republic of China, International Joint Research Center for Animal Disease Prevention and Control of Sichuan Province, Key Laboratory of Animal Disease and Human Health of Sichuan Province, Research Center of Avian Disease and Institute of Veterinary Medicine and Immunology, College of Veterinary Medicine, Sichuan Agricultural University, Chengdu 611130, China.
E-mail address: chenganchun@vip.163.com (A. Cheng).
[1] These authors contributed equally to this work.

https://doi.org/10.1016/j.psj.2025.105336
Received 31 March 2025; Accepted 25 May 2025
Available online 26 May 2025

et al., 2016; Qi, et al., 2009). Currently, as there are no specific antiviral drugs available for DPV and vaccines cannot provide complete protective efficacy, understanding the interactions between the virus and its host and elucidating the viral pathogenesis are the basis for preventing disease outbreaks. In our previous research, DPV has been shown to inhibit innate immune responses in various primary duck cell types (Tian, et al., 2019), but the molecular mechanisms underlying this inhibition remain elusive.

DPV is an enveloped, double-stranded DNA virus composed of four components: unique long (UL), unique short (US), internal repeated sequence (IRS), and terminal repeated sequence (TRS) (You, et al., 2017). The virus encodes a serine/threonine protein kinase (US3) from the US sequence, homologous to the HSV-1 US3 protein, which has been implicated in cell-to-cell spread and virion nuclear egress (Deng, et al., 2020). The US3 kinase in Alpha herpeviridae subfamily members contain minimal consensus phosphorylation sequence (R)n-X-(S/T)-Y-Y, where n≥2, X may be absent or be Arg, Ala, Val, Pro, or Ser, and Y can be any amino acid except proline or an acidic residue (Benetti and Roizman, 2004; Leader, 1993; Leader, et al., 1991; Purves, et al., 1986). Many phosphorylated substrates have been identified for HSV-1, BoHV-1, and other alphaherpesviruses (Jansens, et al., 2017; Kato, et al., 2014; Rao, et al., 2011; Xiong, et al., 2015; Zhang, et al., 2019), the phosphorylation function of DPV US3 kinase also plays a significant role in the process of DPV infection. DPV US3 targets pUL31 and regulates the localization of pUL31/pUL34 to promote nucleocapsids egress through its kinase activity (Deng, et al., 2023). DPV US3 regulates the phosphorylation of UL47 and promotes the cytoplasmic localization of UL47 at the late stage of infection (Deng, et al., 2022). Targeted inhibition of US3 kinase activity with BX795, a kinase inhibitor, inhibited DPV infection in DEF (Tian, et al., 2023). However, whether DPV US3 kinase targets host molecules and the effect on viral pathogenicity is currently unknown.

Innate immune responses are conserved defense mechanisms against viral invasion. Upon viral infection, the host cell promptly initiates antiviral responses after pattern recognition receptors (PRRs) detect virus-derived pathogen-associated molecular patterns (PAMPs). cGAS (cyclic GMP–AMP synthase) is a key cytosolic DNA sensor that detects microbial DNA and induces type I IFN production (Chen, et al., 2016). cGAS synthesizes cGAMP, a second messenger that binds to the adaptor protein STING and induces a conformational change in the STING dimer (Ishikawa and Barber, 2011; Wu, et al., 2013). It recruits TBK1 and activates the transcription factor IFN regulatory factor 3 (IRF3) or IRF7, further stimulating type I IFN production and the synthesis of antiviral proteins for effective defense against pathogens. STING is an ER adaptor, and ER retention/retrieval sequences are critical for maintaining STING dimerization integrity (Ishikawa and Barber, 2008; Sun, et al., 2009). ER exit and STING translocation are pivotal for activating the cGAS/STING signaling pathway (Dobbs, et al., 2015; Zhang, et al., 2020).

To complete invasion and infection of host cells, viruses must overcome the host's antiviral response. Previous studies have shown that many proteins of herpesviruses target the cGAS/STING pathway to inhibit innate immunity. HSV-1 UL24 inhibit the DNA sensing pathway by targeting IRF3 (Xu, et al., 2017). HSV-1 VP22 interacts with cGAS and inhibits the enzymatic activity of cGAS, reducing the production of IFN-β mediated by cGAS/ STING (Huang, et al., 2018). PRV UL21 inhibits the innate immunity by triggering cGAS degradation through autophagy (Ma, et al., 2023) HSV-1 VP1/2 abrogates NF-κB activation in the cGAS/STING signaling pathway by deubiquitinating the K63 linkage of STING, blocking type I interferon expression and promoting brain infection (Bodda, et al., 2020). To achieve immune escape from the host, a single viral protein often targets multiple host proteins to evade the antiviral response. HSV-1 UL46 directly associates with STING and TBK1 to block DNA-sensing signaling and inhibit antiviral responses (Deschamps and Kalamvoki, 2017; You, et al., 2019). HSV-1 US3 inhibits the cGAS/STING signaling pathway by targeting IRF3 (Tian, et al., 2018). Recent studies have shown that US3 of DPV can inhibit IFNβ production by targeting DuIRF7 (Liu, et al., 2022a), it is unclear whether and how DPV US3 kinase targets other adaptors to evade the duck cGAS/STING signaling pathway.

In this study, we investigated the role of DPV US3 kinase in inhibiting duck cGAS/STING signaling pathway-mediated antiviral innate immunity. Mechanistically, we demonstrated that DPV US3 interacts with STING and phosphorylates STING at ER-locating sequence, disrupts STING dimerization and promotes its degradation, inhibits TBK1-mediated STING phosphorylation and its molecular interactions. thereby suppressing the innate immune response. Importantly, we demonstrated the contribution of DPV US3 in antagonizing STING signaling in vivo. Our findings revealed an important mechanism by which DPV US3 antagonizes host innate immunity.

Materials and methods

Ethical statement

All animal experiments were conducted in accordance with approved guidelines. Twenty-day-old Peking ducklings were purchased from a DPV-free farm where DPV vaccination was not implemented. All ducks were housed in an animal facility at Sichuan Agricultural University, China. This study was approved by the Committee of Experimental Operational Guidelines and Animal Welfare of Sichuan Agricultural University (approval number SYXK 2019-187).

Viruses and cells

The DPV CHv strain was stored in the laboratory. The recombinant DPV-CHv-GFP, recombinant DPV-CHv-dUS3 (in which the US3 gene was deleted), and recombinant DPV-CHv-US3-Flag strains were constructed, rescued, and characterized using the DPV BAC system. DPV strains were propagated and titrated on duck embryo fibroblasts (DEF). Human embryonic kidney 293T (HEK293T) and DEF cells were cultured at 37°C under 5% CO_2 in Dulbecco's modified Eagle's medium (DMEM; Gibco, USA) supplemented with 10% fetal bovine serum (FBS; Yeasen, China).

Reagents

MG132 (10 μM) and BAF A1 (200 nM) were purchased from MedChem Express. Cycloheximide (CHX, 10μM) and Phosbind acrylamide (F4002) were purchased from ApexBio. Plasmids were transfected into HEK293T cells using Lipofectamine 2000 reagent (Invitrogen). Plasmids were transfected into DEF cells using Hieff Trans™ Liposomal Transfection Reagent (40802ES02, Yeasen Biotech). Anti-Flag (M185-3, 1:5000), anti-Myc (M192-3, 1:5000), and anti-HA (M180-3, 1:5000) antibodies were purchased from Medical and Biological Laboratories Beijing Biotech. Anti-IgG (7074, 1:1000) and anti-phospho- (Ser/Thr) PKA Substrate antibodies (#9621, 1:1000) were purchased from Cell Signaling Technology. Anti-P- (S/T) antibody (Phospho-Ser/Thr-Pro Motif) (ab117253, 1:1000) was purchased from Abcam. Anti-actin (P30002, 1:5000), anti-GAPDH (3F10, 1:5000), and anti-GFP (7G9, 1:5000) antibodies were purchased from AbMart. SureBeads Protein A and G magnetic beads (Bio-Rad) were used for immunoprecipitation. Horseradish peroxidase (HRP)-conjugated secondary antibodies from Boster Biological Technology were used for immunoblotting.

Plasmids

The duck IFN-β luciferase reporter plasmid (pGL-IFN-β-luc), phRL-TK Renilla luciferase plasmid, and shRNA expressing plasmids against NC (shNC) or STING (shSTING) were constructed previously, and the shSTING oligonucleotide sequence is GCAGGAACCTACAGGCTCATT (Chen, et al., 2018). Based on the expression parent plasmid pcaggs and using standard clone techniques, all the eukaryotic expression plasmids

were constructed, including pcaggs-US3-Flag, US3 WT-HA, US3 K126M-HA, US3 D211A-HA, cGAS-Myc, cGAS-HA, TBK1-Myc, TBK1-HA, IRF7-Flag, IRF7-Myc, STING WT-HA, STING WT-Flag, STING 140-382-Myc, STING 1-341-Myc, STING-Myc, STING S86A-Flag, STING S86E-Flag, STING S86A-Myc, STING S86E-Myc, and a series of DPV proteins. All primers used for plasmid construction were synthesized by Tsingke Biotechnology. All the constructed plasmids were analyzed and verified by DNA sequencing.

Animal infection

To eliminate interference from maternal antibodies, seventy-five 20-day-old Peking ducklings were inoculated with DMEM or 10^4 $TCID_{50}$ of DPV-CHv or DPV-CHv-dUS3 via intracerebral injection. At 1 d post-infection, five duck brains were collected for RNA extraction, and the IFN-β, MX, and OASL mRNA levels were determined via qPCR. Three days post-infection, five duck brains were collected for viral DNA extraction and viral genome detection using qPCR targeting the DPV UL30 gene. The survival rates of 15 ducks were monitored for at least 15 days post-infection.

Dual-luciferase reporter gene assay

The duck IFN-β-luciferase reporter plasmid (pGL-IFN-β-luc), and pRL-TK, were co-transfected into DEF cells with various plasmids expressing duck cGAS, STING, mutants of STING, mutants of US3, proteins of DPV, using Hieff Trans™ Liposomal Transfection Reagent according to the instructions provided by the manufacturer. At 36 h post transfection, whole cell lysates were collected and luciferase activity was measured. The luciferase activities were determined with a Dual-GloLuciferase Assay System (Promega, Madison, WI, USA) and normalized based on the Renilla luciferase activity.

RNA isolation and qRT-PCR

Total RNA was extracted from DEF cells or duckling brains using TRIzol Reagent (Invitrogen) according to the manufacturer's instructions. RNA concentration was determined, genomic DNA was removed, cDNA was synthesized using NovoScript Plus All-in-one 1st Strand cDNA Synthesis SuperMix (gDNA Purge) (Novoprotein, Shanghai, China), and qRT-PCR analysis was performed as described previously (Tian, Cai, He, Deng, Wu, Wang, Jia, Zhu, Liu, Yang, Wu, Zhao, Chen, Zhang, Huang, Ou, Mao, Yu, Zhang, Liu and Cheng, 2019). Briefly, cDNA was transcribed from 1 μg of RNA using the Superscript III Reverse Transcription kit. A total of 1 μL cDNA, 3 μL double-distilled water, and 0.5 μL primer for each gene were mixed. The cDNA was amplified using iQ5 SYBR Green (Bio-Rad, Hercules, CA, USA) and forward and reverse primers for each gene, and the cycle threshold (CQ) was recorded. The cDNA concentration, primer concentration, and Q-PCR procedure were consistent for each gene, and the relative mRNA expression was normalized to the expression level of actin mRNA gene (ΔCT CT [PRR or ISG]/ΔCT [actin]). Expression levels of induced mRNAs were presented as the fold-change relative to mock-infection levels according to the 2-ΔΔCT method. Genomic copy numbers of DPV were quantified using an absolute Q-PCR method with primers specific to the DPV UL30 gene. Primers used for Q-PCR as follows: IFN-β F, TCTACAGAGCCTTGCCTGCAT; IFN-β R, TGTCGGTGTCCAAAAGGATGT; MX F, TGCTGTCCTTCATGACTTCG; MX R, GCTTTGCTGAGCCGATTAAC; OASL F, TCTTCC TCAGCTGCTTCTCC; OASL R, ACTTCGATGGACTCGCTGTT; β-actin F, GCCCTCTTCCAGCCATCTTT; β-actin R, CTTCTGCATCCTGTCAGCGA; DPV UL30 F, TTTCCTCCTCCTCGCTGAGTG; DPV UL30 R, CCAGAAACATACTGTGAGAGT; Taqman probe to DPV UL30, CGCTTGTACCCAGGG. All primers used for Q-PCR were synthesized or labeled by Tsingke Biotechnology.

Immunoprecipitation and immunoblot analysis

After transfection or virus infection, cells were lysed with 1% Triton buffer (50 mM Tris HCl pH 7.4, 1 mM EDTA, 150 mM NaCl, 20 mM N-Ethylmaleimide, 1% Triton X-100) supplemented with a protease inhibitor cocktail (Sigma), followed by centrifugation at 12,000 g for 15 min at 4°C. The supernatants were incubated with anti-Flag, Myc, or HA affinity beads or the indicated antibodies, followed by incubation with protein A/G agarose beads. Immunoprecipitated proteins were washed at least five times with 1% Triton buffer. Cell lysates or immunoprecipitates were separated by SDS-PAGE and transferred onto a PVDF membrane (Bio-Rad). The membranes were then incubated with appropriate primary and secondary antibodies and visualized using a Bio-Rad system (Bio-Rad, Germany).

Statistical analysis

Results were presented as means ± SEM. For statistical analysis, GraphPad Prism Software 6 (La Jolla, CA, USA) was used. One-way ANOVAs followed by Tukey's post hoc test were utilized for multiple group comparisons of the parameters. Differences in survival curves of ducks were analyzed by Mantel-Cox test. Differences in the frequencies of histology scores were analyzed by the Mann-Whitney test. Graphs are presented as means ± SEM, data are representative of three independent experiments, * P <0.05; ** P <0.01; *** P<0.001: **** P<0.0001.

Results

DPV US3 inhibits the cGAS/STING signaling pathway

Our previous study demonstrated that DPV suppresses the antiviral innate immune response after infection in various types of duck primary cells (Tian et al., 2019). To further investigate the mechanism by which DPV inhibits the antiviral immune response, we infected DEF cells with 1 MOI of DPV-CHv strain and monitored interferon beta (IFN-β) mRNA levels at various time points post-infection (Fig. 1A). We observed that IFN-β was slightly upregulated early after DPV infection, but gradually downregulated and lower than in control cells at 24 hpi (Fig. 1A), demonstrating DPV's inhibitory effect on antiviral immunity. To identify which DPV gene inhibits IFN-β expression, we transfected a dual luciferase reporter plasmid containing a duck IFN-β promoter into DEF cells along with cGAS and STING expression plasmids, as well as multiple DPV protein expressing plasmids. The results indicated that IFN-β was stimulated by duck cGAS and STING, and approximately 36 DPV proteins inhibited IFN-β induction, including gI, gE, UL7, US1, UL49, ICP4, and US3 (Fig. 1B). DPV US3 exhibited the strongest inhibitory activity among the DPV proteins (Fig. 1B), suggesting that it plays a critical role in inhibiting innate immune responses. We further validated the inhibitory effect of DPV US3 on IFN-β expression induced by cGAS+STING using qPCR assays. IFN-β and MX mRNA were stimulated by cGAS+STING and significantly inhibited by DPV US3 (Fig. 1C and D). These data suggest that DPV US3 is a potential inhibitor of the antiviral innate immune response mediated by the duck cGAS/STING pathway.

DPV US3 protein kinase interacts with duck STING

To determine the molecular mechanism by which DPV US3 protein kinase regulates cGAS/STING signaling activity, co-immunoprecipitation (CoIP) assays were used to clarify their interaction. When Flag-STING or Flag-IRF7 were co-transfected with HA-US3, US3 was precipitated from whole cell lysates using an anti-HA-primary antibody. We found that US3 obviously precipitated with STING, but not with IRF7 (Fig. 2A), and did not precipitate cGAS and TBK1 (Fig. 2B and C). When HA-US3 and Flag-STING were co-transfected into DEF cells and the cell lysates incubated with an anti-Flag antibody, we found that STING precipitated US3 (Fig. 2D). We

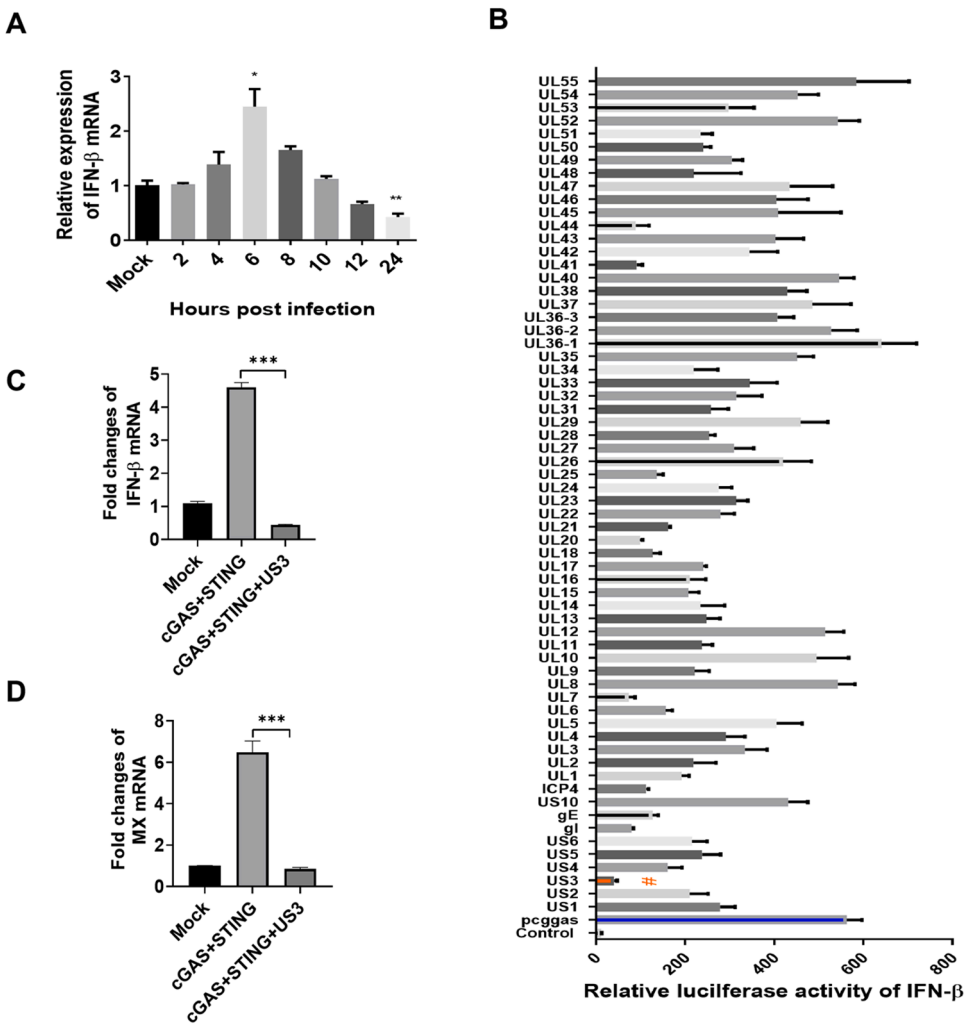

Fig. 1. DPV US3 inhibits the cGAS/STING signaling pathway. (A) The DEF cells were infected with 1 MOI of DPV CHv strain, the IFN-β mRNA was determined through Q-PCR method. (B) The DEF cells were transfected with duck IFN-β luciferase reporter gene, phRL-TK Renilla luciferase plasmid, cGAS and STING expression plasmids, together with DPV proteins expression plasmids, the luciferase activity was measured 36 hours after transfection and normalized to renilla luciferase activity. (C and D) The DEF cells were transfected with cGAS and STING expression plasmids, together with DPV US3 expression plasmid, the mRNA of IFN-β and MX were measured 24 hours after transfection through Q-PCR method. Graphs are presented as means ± SEM, data are representative of three independent experiments, $^{*}P < 0.05$; $^{**}P < 0.01$; $^{***}P < 0.001$; $^{****}P < 0.0001$ (t test or One-way ANOVAs followed by Tukey's post hoc test for A, B, C, and D).

next investigated the interaction between US3 and STING proteins during viral infection. DEF cells were pre-transfected with Myc-STING expression plasmid, infected with the DPV-CHv-US3-Flag strain, and then CoIP assays were performed using anti-Flag or anti-Myc antibodies. The result showed a physical interaction between US3 and STING proteins (Fig. 2E and 2F), indicating that US3 binds to STING during DPV infection. These data demonstrate that US3 specifically interacts with STING.

DPV US3 reduces STING dimerization and induces STING degradation

To investigate the mechanism by which DPV US3 inhibits STING-mediated antiviral immune responses, we tested whether US3 affects STING stability. HEK293T cells were transfected with STING or TBK1 expression plasmids, along with the DPV US3 expression plasmid (Fig. 3A). The protein level of STING, but not TBK1, was significantly reduced in the presence of DPV US3 compared to control cells (Fig. 3A). The transcription level of STING did not change upon US3 overexpression (data not shown), indicating that DPV US3 affects STING stability at the protein level. To verify whether STING degradation depends on DPV US3, we performed a protein-chase experiment. When protein translation was blocked by the addition of the translation inhibitor cycloheximide (CHX), STING was degraded upon US3 overexpression (Fig. 3B), indicating that DPV US3 induces STING degradation. To determine the cellular STING degradation pathway, we examined the proteasome and autolysosomal degradation pathways, the two main pathways involved in cellular protein disposal. When the proteasome or autolysosome degradation pathways were blocked by the inhibitors MG132 or BAF A1, respectively, US3-induced STING degradation was recovered in both cases (Fig. 3C), indicating that US3 induces STING degradation through these pathways. To further investigate whether DPV infection induces STING degradation, DEF cells were transfected with the Myc-STING expression plasmid and then infected with the DPV-CHv-WT-GFP strain or the DPV-CHv-dUS3-GFP strain (recombinant virus with deleted US3 gene). The STING protein level decreased or even disappeared in DPV-CHv-WT-GFP-infected cells but partially recovered in DPV-CHv-dUS3-GFP-infected cells (Fig. 3D). These results suggest that DPV infection induced STING degradation may be caused by US3 protein.

To determine whether US3 affects STING dimerization, Flag-STING and Myc-STING expression plasmids were transfected into HEK293T cells along with varying doses of the HA-US3 expression plasmid, and

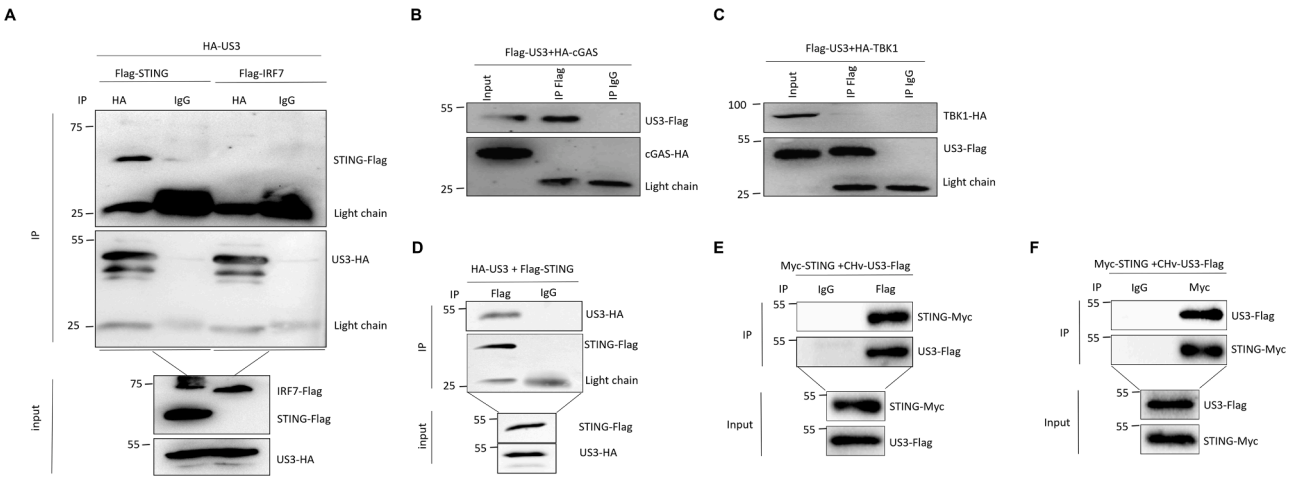

Fig. 2. DPV US3 protein kinase interacts with duck STING. (A) HEK293T cells were transfected with duck Flag-STING or Flag-IRF7 expression plasmids, together with DPV HA-US3 expression plasmid for 36 hours, then the whole cell lysates (WCLs) were collected and part of WCLs were used for CoIP against HA and immunoblot assays. (B and C) HEK293T cells were transfected with duck HA-cGAS, or HA-TBK1 expression plasmids, together with Flag-US3 expression plasmid for 36 hours. The WCLs were used for CoIP against Flag and immunoblot assays. (D) DEF cells were transfected with HA-US3 and Flag-STING expression plasmids for 36 hours. The WCLs were used for CoIP against Flag and immunoblot assays. (E and F) DEF cells were transfected with Myc-STING expression plasmid for 12 hours, then the DEF cells were infected with 1 MOI of DPV-CHv-US3-Flag for 36 hours, then the WCLs were used for Co-IP against Flag or Myc and immunoblot assays.

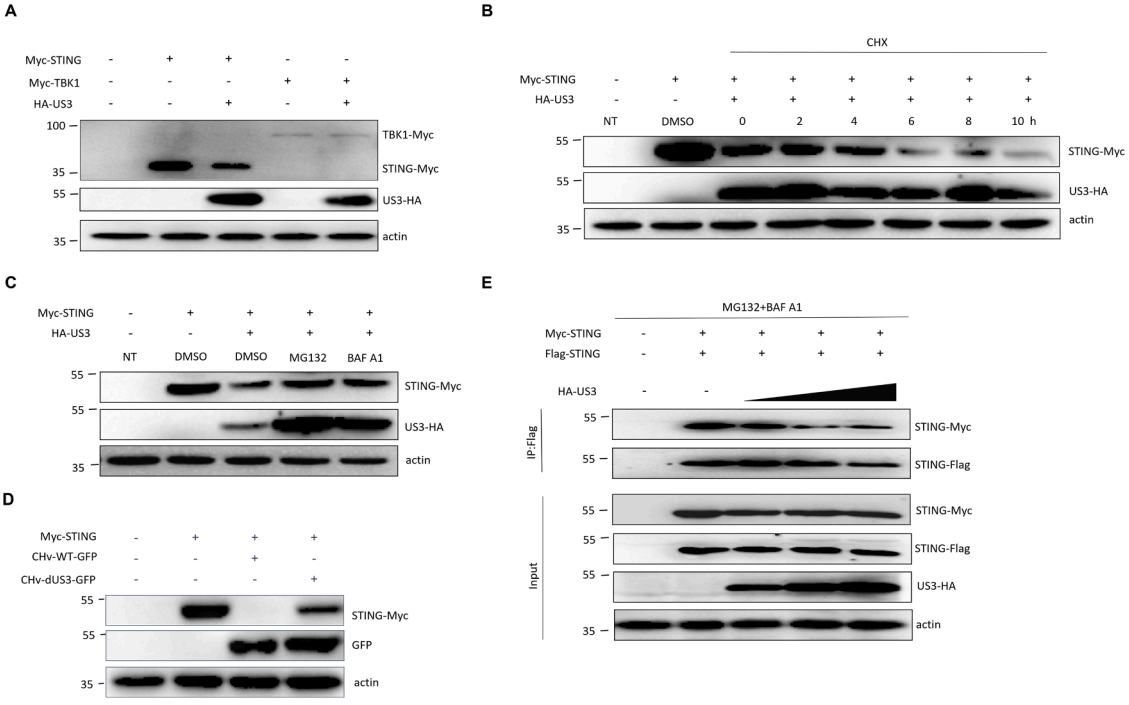

Fig. 3. DPV US3 reduces STING dimerization and induces STING degradation. (A) DEF cells were transfected with duck Myc-STING, and Myc-TBK1 expression plasmids, together with pcaggs or pcaggs-HA-US3 plasmids for 36 hours. The proteins level of duck STING, TBK1, US3, and actin were characterized through immunoblot assays. (B) DEF cells were transfected with duck Myc-STING expression plasmid, alone or together with DPV HA-US3 expression plasmid for 24 hours, respectively. Then the CHX (20 μM) was added and WCLs were collected at the indicated time and used for immunoblot assays. (C) DEF cells were transfected with duck Myc-STING expression plasmid, alone or together with DPV HA-US3 expression plasmid for 36 hours, respectively. Then MG132 (10 μM) and BAF A1 (20 μM) were added for 6 hours and the WCLs were extracted and used for immunoblot assays. (D) The DEF cells were transfected with duck Myc-STING expression plasmid for 12 hours and infected with 1 MOI of DPV-CHv-WT-GFP strain or DPV-CHv-dUS3-GFP strain for 36 hours, then the WCLs were collected for immunoblot assays. (E) HEK293T cells were transfected with indicated plasmids for 36 hours and MG132 and BAF A1 were added for 6 hours, then the WCLs were used for CoIP against Flag and immunoblot assays.

CoIP assays were performed using an anti-Flag antibody (Fig. 3E). We observed that Myc-STING co-precipitated with Flag-STING, demonstrating that STING was fully dimerized (Fig. 3E). However, in the presence of DPV US3, Myc-STING co-precipitated with Flag-STING gradually decreased in a dose-dependent manner, suggesting that US3 disrupts STING dimerization (Fig. 3E). These data demonstrate that DPV US3 induces the degradation of STING through the proteasome and autolysosome pathways, thereby reducing the stability and dimerization level of STING.

The kinase activity of DPV US3 is indispensable for STING degradation and inhibition of STING mediated antiviral immune responses

The US3 protein is a conserved protein kinase in the Alphaherpesvirinae subfamily; however, the kinase activity and dominant amino acid sites of the DPV US3 protein have not been characterized. We aligned the DPV US3 amino acid sequence with those of US3 from herpes simplex virus type 1 (HSV-1), bovine herpesvirus 1 (BoHV-1), pseudorabies virus (PRV), and Marek's disease virus (MDV), and found that two key kinase activity sites (K126 and D211) were conserved across these viruses (data not shown). It has been reported that the specific target of US3 phosphorylation is similar to that of protein kinase A (PKA), and the US3 phosphorylated substrate can also be recognized by a phospho- (Ser/Thr) PKA substrate antibody (Benetti and Roizman, 2004), Therefore, we constructed two DPV US3 kinase-dead mutant expression plasmids (US3 K126M and US3 D211A) and validated US3 kinase activity using a phospho- (Ser/Thr) PKA substrate antibody. Higher signals recognized by the phospho- (Ser/Thr) PKA substrate antibody under overexpression of US3, but these signals were reduced in the kinase-dead mutant US3 K126M and US3 D211A overexpressing cells as compared to mock cells (Fig. 4A). This suggests that DPV US3 is a typical protein kinase and that its conserved active sites are K126 and D211. To verify whether duck STING is phosphorylated by DPV US3, we transfected Myc-STING together with HA-US3 or its kinase-dead mutants HA-US3-K126M and HA-US3-D211A in 293T cells, and the phosphorylation of STING was detected with an anti-P- (S/T) antibody (Phospho-Ser/Thr-Pro Motif) after IP with Myc antibody (Li, et al., 2019). Significantly phosphorylated STING was observed in US3-expressing cells, but not in those expressing US3-K126M or US3-D211A (Fig. 4B), indicating that STING is phosphorylated by DPV US3 protein kinase and depends on its kinase activity. Furthermore, we co-transfected the duck Myc-STING expression plasmid with HA-US3,

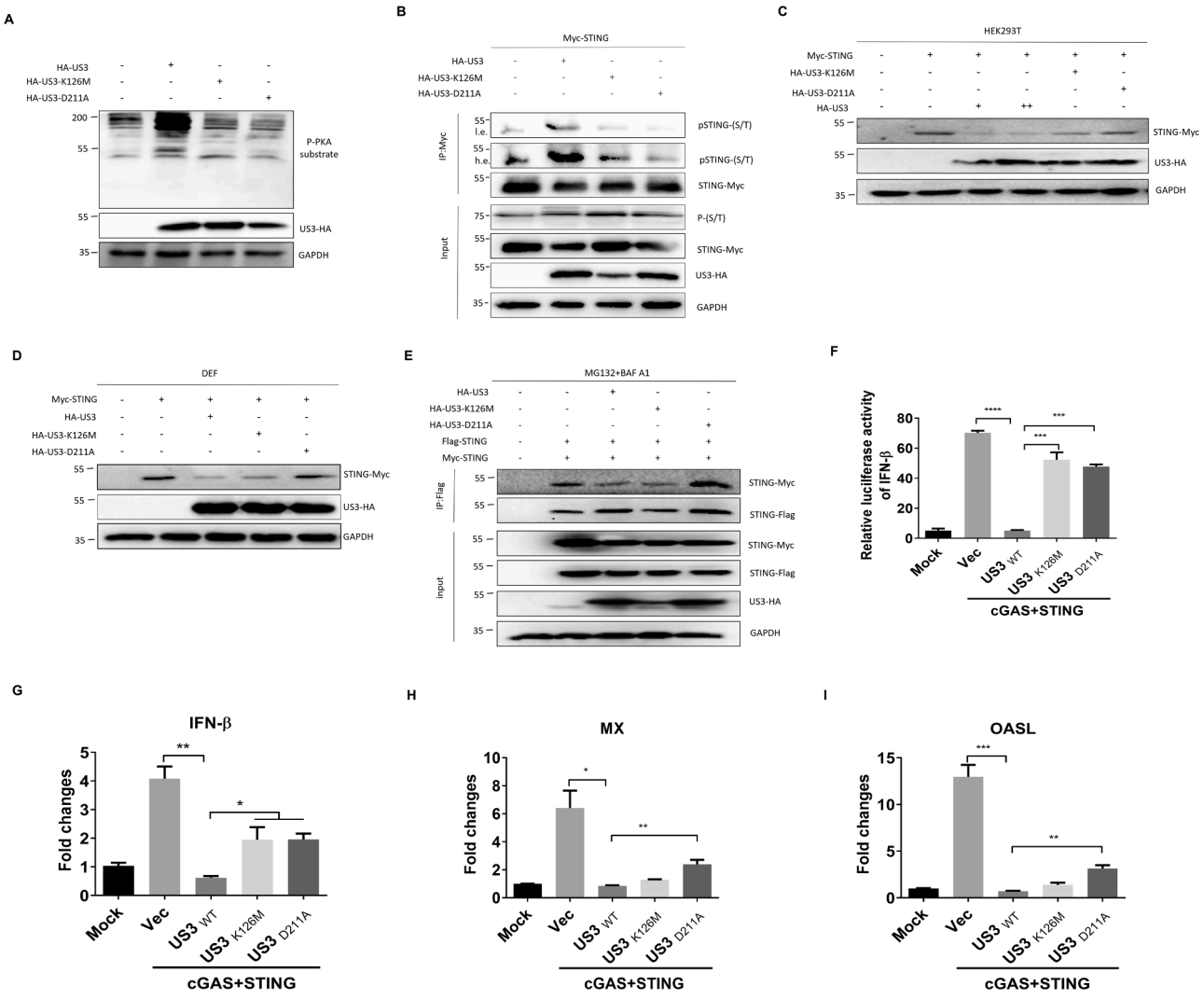

Fig. 4. The kinase activity of DPV US3 is indispensable for STING degradation and inhibition of STING mediated antiviral immune responses. (A) DEF cells were transfected with indicated plasmids for 36 hours and the WCLs were extracted and used for immunoblot assays with Phospho- (Ser/Thr) PKA substrate antibody, HA and GAPDH primary antibodies. (B) DEF cells were transfected for 36 hours and added MG132 and BAF A1 for 6 hours, then the WCLs were used for CoIP against Myc and immunoblot assays. (C and D) HEK293T cells and DEF cells were transfected with indicated plasmids for 36 hours and the WCLs were extracted and detected via immunoblot assays. (E) HEK293T cells were transfected with duck Myc-STING expression plasmid, alone or together with DPV HA-US3 and its kinase activity mutants expression plasmids for 36 hours, and added MG132 and BAF A1 for 6 hours, then the WCLs were used for CoIP against Flag and immunoblot assays. (F) The DEF cells were transfected, and the luciferase activity was measured 36 hours after transfection and normalized to renilla luciferase activity. (G-I) The DEF cells were transfected with the indicated plasmids for 24 hours and the IFN-β, MX, and OASL mRNA level were measured by Q-PCR assays. Graphs are presented as means ± SEM, data are representative of three independent experiments, $^{*}P < 0.05$; $^{**}P < 0.01$; $^{***}P < 0.001$; $^{****}P < 0.0001$ (One-way ANOVAs followed by Tukey's post hoc test for the rest for F-I).

HA-US3-K126M, or HA-US3-D211A expression plasmids into HEK293T and DEF cells and found that the kinase-dead mutant HA-US3 D211A did not induce STING degradation in either cell type (Fig. 4C and D), indicating that the kinase activity of DPV US3 is important for inducing STING degradation. We investigated whether US3 kinase activity affects STING dimerization. HEK293T cells were transfected with Flag-STING and Myc-STING expression plasmids together with HA-US3 and its enzyme-active mutants K126M, D211A. Anti-Flag antibody was used to precipitate Flag-STING, and we observed that US3-WT, but not US3-D211A mutants, inhibited STING dimerization (Fig. 4E), implying that DPV US3 kinase destruction of STING dimerization is kinase activity-dependent.

Next, we explored whether DPV US3 kinase activity affects STING mediated antiviral immune responses, luciferase assays demonstrated that overexpression of US3 WT significantly inhibited cGAS+STING stimulated IFN-β promoter luciferase reporter activity, but the US3 kinase death mutants (US3 K126M and US3 D211A) attenuated this effect (Fig. 4F). Similarly, duck cGAS+STING overexpression enhanced mRNA levels of duck IFN-β and ISGs, which were inhibited by DPV US3 WT expression but not by kinase-dead mutants US3 K126M and US3 D211A (Fig. 4G-I). These data illustrate that the DPV US3 kinase activity is indispensable for blocking STING-mediated antiviral immune responses.

STING S86A mutant resists to US3 kinase induced degradation

Human STING is an endoplasmic reticulum membrane protein that contains four transmembrane helices, followed by a cytoplasmic ligand-binding and signaling domain (Gao, et al., 2013). However, the transmembrane and functional domains of the duck STING remain unclear. We analyzed the transmembrane domains of duck STING using TMpred (http://www.ch.embnet.org/software/TMPRED_form.html) (Fig. 5A) and aligned the amino acid sequences of duck STING with those of human STING. To map the interaction domain of duck STING with DPV US3 kinase, we constructed two mutants of duck STING expression

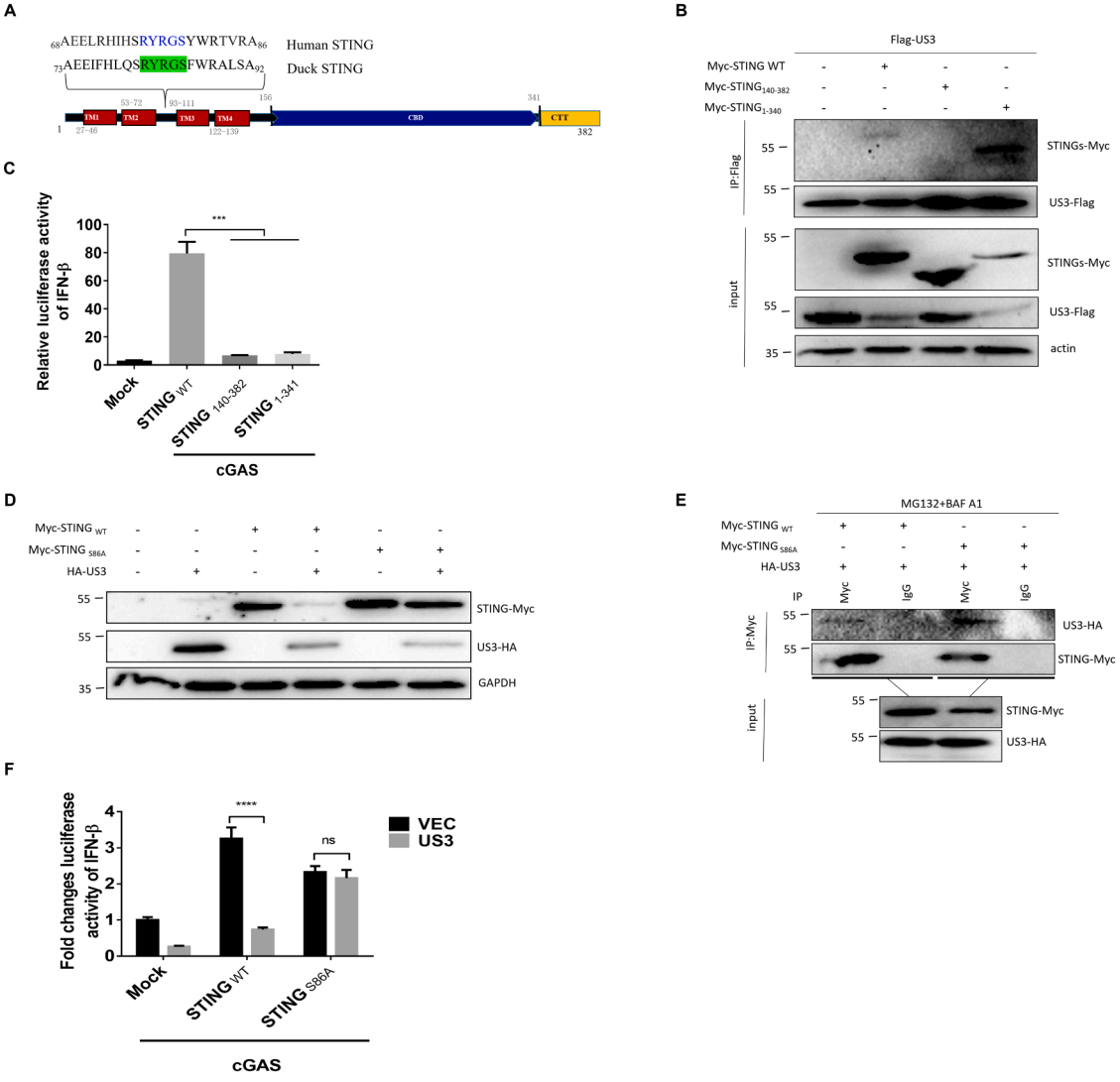

Fig. 5. STING S86A mutant resistant to US3 kinase induced degradation. (A) Schematic and sequence align of duck STING. (B) HEK293T cells were transfected with indicated plasmids for 36 hours and added MG132 and BAF A1 for 6 hours and the WCLs were used for CoIP against Flag and immunoblotting assays. (C) The DEF cells were transfected and the luciferase activity was measured 36 hours after transfection and normalized to renilla luciferase activity. (D) DEF cells were transfected and the WCLs were extracted 36 hours after transfection and used for immunoblotting assays against Myc, HA, and GAPDH antibodies. (E) HEK293T cells were transfected with indicated plasmids for 36 hours and added BAF A1 for 6 hours and the WCLs were extracted and used for CoIP against Myc antibody and immunoblotting assays. (F) The DEF cells were transfected, and the luciferase activity was measured 36 hours after transfection and normalized to renilla luciferase activity. Graphs are presented as means ± SEM, data are representative of three independent experiments, $^{*}P < 0.05$; $^{**}P < 0.01$; $^{***}P < 0.001$; $^{****}P < 0.0001$ (One-way ANOVAs followed by Tukey's post hoc test for the rest for F).

plasmids, Myc-STING 140-382 (TMs deletion) and Myc-STING 1-341 (C terminal tail (CTT) deletion), with deletion of 1-140 aa or 342-382 aa, respectively. Myc-STING WT, Myc-STING 140-382, and Myc-STING 1-341 were co-transfected with Flag-US3. We then performed a CoIP experiment using an anti-Flag antibody and observed that STING WT and STING 1-341 was precipitated by Flag-US3, but STING 140-382 did not (Fig. 5B), suggesting that the N-terminal TMs of STING are pivotal for its interaction with DPV US3. We further verified the stimulatory effects of STING WT, STING 140-382 and STING 1-341 on innate immunity. We observed that duck STING WT significantly enhanced IFN-β expression (Fig. 5C), but STING 140-382 and STING 1-341 did not, suggesting that both N terminal TMs (1-140 aa) and CTT (342-382 aa) domain of duck STING are indispensable for mediating antiviral responses.

Although US3 kinase mainly recognizes the minimal consensus phosphorylation sequence (R)n-X- (S/T)-Y-Y (Benetti and Roizman, 2004; Wang, et al., 2011), this strict sequence is absent in the duck STING sequence. However, we found that there is a short mimic sequence between the TM2 and TM3, "R_{82}YRGS_{86}," equivalent to the human STING (Fig. 5A), maybe the potential target of DPV US3. To test this hypothesis, we constructed a STING S86A mutant and overexpressed it using DPV US3 kinase. We observed that STING S86A mutants were more resistant to DPV US3 kinase-induced degradation than WT STING (Fig. 5D). However, the CoIP assays showed that both STNG WT and STING S86A precipitated with DPV US3 kinase, suggesting that STING S86 is not essential for the interaction with DPV US3 (Fig. 5E). Additionally, DPV US3 antagonized STING WT-mediated IFN production but not STING S86A-mediated IFN production (Fig. 5F). Altogether, these data demonstrated that US3 may recognize serine in the "R_{82}YRGS_{86}" amino acid sequence of duck STING to inhibit the innate immunity.

DPV US3 kinase disrupts association and phosphorylation between STING and TBK1

During human STING activation, the conserved PLPLRT/SD motif of STING mediates the recruitment and activation of TBK1. STING is then phosphorylated at S366 by TBK1 on the pLxIS motif (Liu, et al., 2015; Tanaka and Chen, 2012; Zhao, et al., 2019). After aligning the duck STING CTT with that of human STING, we found that these motifs and key sites were conserved in the duck STING CTT (Fig. 6A). There are no reports confirming that duck STING is associated with and phosphorylated by TBK1 and there is no suitable antibody to test TBK1 phosphorylated duck STING. To address these questions, we constructed two mutants: STING S369A and STING L377A. In the presence of duck TBK1, duck STING WT obviously lagged in the SDS-PAGE and immunoblotting assays, demonstrating that duck STING is phosphorylated by TBK1 (Fig. 6B). However, lagged STING was reduced in STING S369A and almost disappeared in STING L377A (Fig. 6B), confirming that duck TBK1 was associated with duck STING via the PQPLRSD motif, and phosphorylated duck STING at S369 via the pLQIS motif. We further compared mutant STING S86A and the phosphorylating mimic mutant STING S86E with WT STING in the presence of TBK1 and found that these two mutants had no significant effect on the phosphorylated STING of TBK1 (Fig. 6B). Using the duck IFN-β luciferase reporter assays, we found that duck STING mediated IFN-β was abolished in mutant STING S369A and STING L377A, and attenuated in mutant STING S86A (Fig. 6C), confirming the importance of STING S369 and L377.

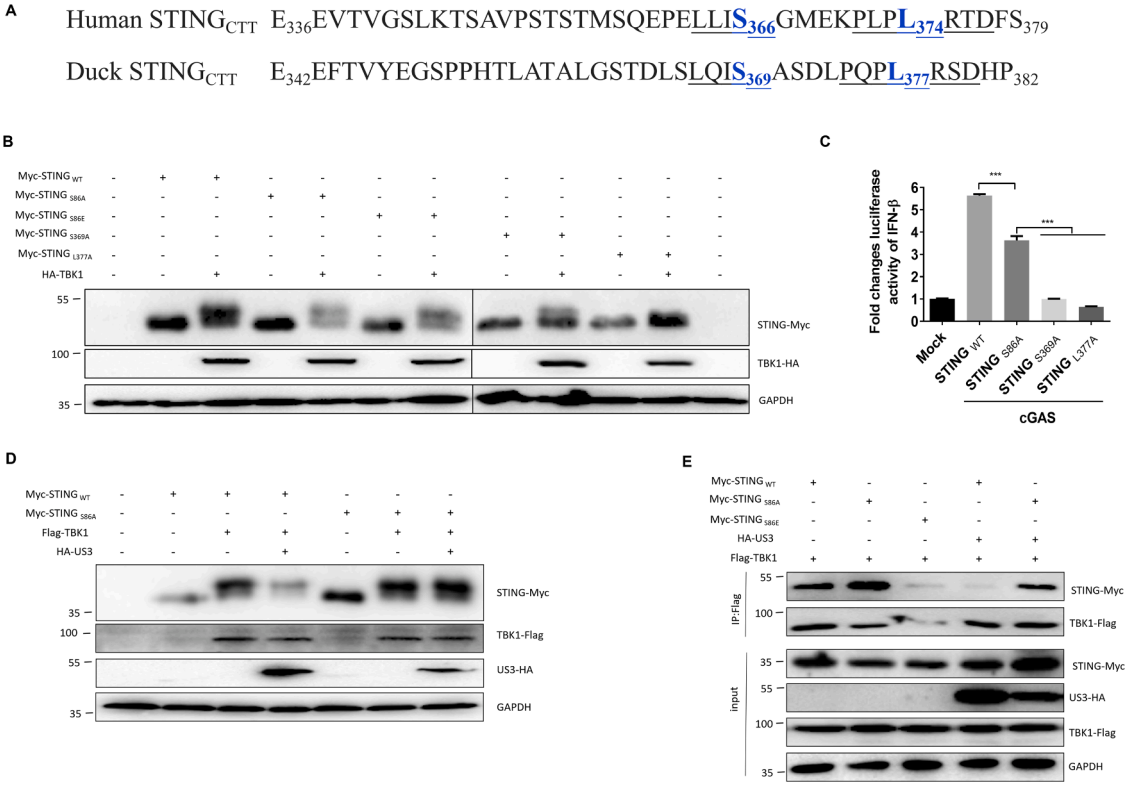

Fig. 6. US3 kinase disrupts the interaction between STING and TBK1, and phosphorylation of STING mediated by TBK1. (A) Alignment of the duck STING CTT with human STING CTT. (B) HEK293T cells were transfected with indicated plasmids for 36 hours and the WCLs were used for immunoblotting assays. (C) The DEF cells were transfected, and the luciferase activity was measured 36 hours after transfection and normalized to renilla luciferase activity. (D) HEK293T cells were transfected with the indicated plasmids for 36 hours, then the WCLs were used for immunoblotting assays. (E) HEK293T cells were transfected with the indicated plasmids for 36 hours and added BAF A1 for 6 hours and the WCLs were used for CoIP against Flag antibody and immunoblotting assays. Graphs are presented as means ± SEM, data are representative of three independent experiments, $^{*}P < 0.05$; $^{**}P < 0.01$; $^{***}P < 0.001$; $^{****}P < 0.0001$ (One-way ANOVAs followed by Tukey's post hoc test for the rest for C).

Furthermore, this may suggest that STING S86 is another key site for duck STING activation by TBK1, similar to STING S358 in humans (Zhong, et al., 2008). We validated the presence of DPV US3 kinase disrupts the phosphorylation and association between duck TBK1 and duck STING WT. However, DPV US3 kinase did not affect the phosphorylation or association between duck TBK1 and the duck STING S86A mutant (Fig. 6D and E). Furthermore, the phospho-mimic mutant STING S86E showed impaired interaction with TBK1 (Fig. 6E). Taken together, these results demonstrate that DPV US3 competitively phosphorylates duck STING S86 to disrupt the phosphorylation and association between duck STING and TBK1.

DPV US3 suppresses STING-mediated antiviral innate immune response

To verify whether DPV US3 inhibits the STING-mediated innate immune response under viral infection conditions, we used a previously identified shRNA against STING to knock down STING expression in DEF (Chen, Wu, Zhang, Wang, Jia, Zhu, Liu, Sun, Yang, Wu, Zhao and Cheng, 2018), infected with the parent DPV-CHv strain and the previously constructed recombinant DPV-CHv-dUS3 strain (Deng, Wang, Cheng, Yang, Wu, Jia, Chen, Zhu, Liu, Zhao, Zhang, Huang, Ou, Mao, Zhang, Liu, Yu, Tian, Pan, Rehman and Chen, 2020). The DEF cells were transfected with shNC or shSTING expression plasmid, then infected with 1 MOI of parent DPV-CHv or DPV-CHv-dUS3 strain, respectively, and the IFN-β mRNA expression was determined at 24 hpi after infection (Fig. 7A). The IFN-β expression was higher in shNC transfected and DPV-CHv-dUS3 infected DEF cells compared to DPV-CHv and mock infected DEF cells (Fig. 7A). However, the IFN-β expression in the DPV-CHv-dUS3 infected cells was significantly reduced after STING was knocked down (Fig. 7A). These results suggest that DPV utilizes US3 to antagonize duck STING-mediated antiviral innate immune responses. To further verify the role of DPV US3 in resistance to STING-mediated antiviral innate immunity, DEF were pre-transfected with shSTING to knock down STING expression and then infected with DPV-CHv or DPV-CHv-dUS3 strains. The results showed that viral genome replication of the DPV-CHv-dUS3 strain was significantly enhanced in STING knockdown DEFs compared to that of the DPV-CHv strain (Fig. 7B). The number of released viruses in cell culture by both strains increased at 12 hpi after STING knockdown, but the increase in the virus titer of DPV-CHv-dUS3 at 24 hpi was significantly higher than that of DPV-CHv (Fig. 7C). These results demonstrate that DPV US3 inhibits STING-mediated antiviral innate immune response.

The pathogenicity of DPV-CHv-dUS3 is weakened in ducklings

To investigate whether US3 affects the pathogenicity of DPV, we conducted an animal infection experiment (Fig. 7D), in which ducklings were inoculated with 10^4 $TCID_{50}$ of the DPV-CHv or DPV-CHv-dUS3 strains through intracranial injection. Post-injection the antiviral innate response, viral load, and survival of ducklings were monitored (Fig. 7E-I). The mRNA levels of IFN-β, 2′-5′-oligoadenylate synthetase like (OASL) and Myxovirus resistance (MX) in brain tissues of duckling infected with DPV-CHv-dUS3 strain were significantly higher than those of duckling infected with DPV-CHv strain (Fig. 7E-G). In addition, the

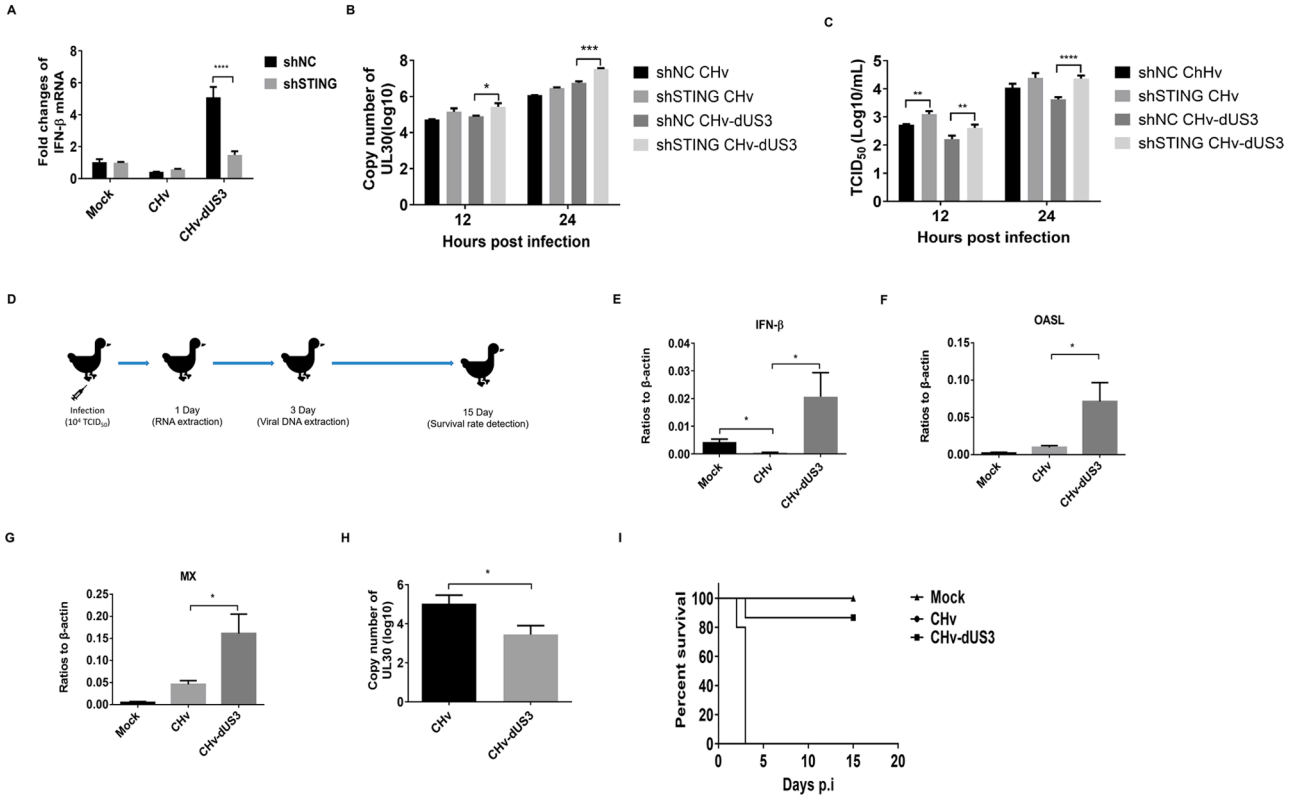

Fig. 7. DPV US3 antagonizes the STING mediated innate immune responses and promotes DPV replication *in vitro* and pathogenicity *in vivo*. (A) DEF cells were transfected with shNC or shSTING expression plasmids for 12 hours, then the cells were infected with 1 MOI of DPV-CHv or DPV-CHv-dUS3 for 24 hours, the cells were collected for RNA extraction and the IFN-β mRNA level was measured via Q-PCR assays. (B) DEF cells were pre-transfected with shRNA for 12 hours and infected with DPVs and the cells were collected at the indicated time for viral DNA extraction and viral load study. (C)The cell culture supernatants were collected and used for viral titer determination through $TCID_{50}$ assays. (D) Flow chart of animal experiments. (E-G) 5 duck brains were collected 1 day after infection for RNA extraction and the IFN-β, MX, and OASL mRNA level were determined via Q-PCR method. (H) 5 duck brains were collected 3 days after infection for viral DNA extraction and viral genome level detection via Q-PCR method targeting DPV UL30 gene. (I) The survival ratios of 15 ducks were monitored at least for 15 days after DPV-CHv or DPV-CHv-dUS3 inoculation. Graphs are presented as means ± SEM, data are representative of three independent experiments, $^*P < 0.05$; $^{**}P < 0.01$; $^{***}P < 0.001$; $^{****}P < 0.0001$ (Mantel-Cox test for I, One-way ANOVAs followed by Tukey's post hoc test for the rest for A-C and E-H).

viral load was lower in DPV-CHv-dUS3 strain infected duckling brain infected with DPV-CHv (Fig. 7H). We then monitored the survival of ducklings after infection and found that approximately 86% of the ducklings survived infection with the DPV-CHv-dUS3 strain, but all ducklings died within 3 days after infection with the DPV-CHv strain (Fig. 7I). These results indicate that US3-induced inhibition of duck STING-mediated innate antiviral responses is indispensable for DPV pathogenicity *in vivo*.

Discussion

DPV causes the highest mortality among Alphaherpesviridae members; however, the molecular mechanism of antiviral immunity evasion remains unexplored. STING is a direct innate immune sensor of cyclic dinucleotides (CDNs) that regulate antiviral immunity against viral infections (Burdette, et al., 2011). In this study, we found that DPV US3 strongly inhibits host antiviral immunity. DPV US3 interacts with duck STING and phosphorylates STING at a serine residue near the ER retention sequence, disrupting the association and phosphorylation of STING and TBK1, impairing STING dimerization, reducing STING stability, and inducing STING degradation through proteasome and autolysosome pathways, ultimately blocking STING-mediated IFN production. To our knowledge, this is the first report demonstrating that a US3 kinase from the Alphaherpesviridae subfamily can directly target STING to counteract innate immune responses.

US3 kinase of the Alphaherpesviridae subfamily is a strong antiviral immunity inhibitor with multiple targets. For example, HSV-1 US3 kinase phosphorylates the Bcl family member BAD and blocks apoptosis (Cartier, et al., 2003; Ogg, et al., 2004). HSV-2 US3 kinase disrupts promyelocytic leukemia protein nuclear bodies (PML-NBs) in a kinase- and proteasome-dependent manner (Jung, et al., 2011). HSV-1 US3 also phosphorylates interferon regulatory factor 3 (IRF3), nuclear factor kappa B (NF-κB), and β-catenin to block the DNA-sensing pathway mediated antiviral immunity (Wang, et al., 2014; Wang, et al., 2013; You, et al., 2020). Feline Herpesvirus 1 US3 blocks the type I interferon signaling pathway by targeting IRF3 dimerization in a kinase-independent manner (Tian, Liu, Liu, Sun, Zhang and Qu, 2018). DPV US3 inhibits IFNβ production by targeting IRF7 (Liu, et al., 2022b). Whether US3 targets other molecules in the cGAS/STING pathway remains to be investigated. In this study, we screened potential inhibitory genes of DPV on antiviral immunity and identified approximately 36 genes with this capability, of which DPV US3 was the strongest. We further confirmed that DPV US3 affects the stability of duck STING through its interaction with and phosphorylation of STING.

The DPV US3 protein is a predicted conserved kinase within the Alphaherpesviridae subfamily (Benetti and Roizman, 2004; Leader, 1993; Leader, Deana, Marchiori, Purves and Pinna, 1991; Purves, Deana, Marchiori, Leader and Pinna, 1986). However, the kinase activity of DPV US3 has not been directly demonstrated. In this study, we aligned the amino acid sequence of DPV US3 with those of other Alphaherpesviridae members and identified K126, D211, and K213 of DPV US3 as key conserved kinase sites. We confirm that DPV US3 is a kinase and that the predicted sites, K126 and D211, are critical for its kinase activity. We further demonstrated that the kinase activity of US3 is essential for STING phosphorylation, degradation induction, reduction of dimerization, and evasion of STING-mediated antiviral immunity. These data suggest that the DPV US3 kinase targeting STING to evade antiviral immunity may represent a conservative strategy among the Alphaherpesviridae, but further evidence is needed from other subfamily members.

STING is a direct sensor of CDNs that initiates antiviral immunity (Burdette, Monroe, Sotelo-Troha, Iwig, Eckert, Hyodo, Hayakawa and Vance, 2011). The ER retention/retrieval sequences of STING are critical for maintaining STING dimerization, whereas ER exit and translocation are crucial for activating the cGAS/STING signaling pathway (Dobbs, Burnaevskiy, Chen, Gonugunta, Alto and Yan, 2015; Ishikawa and Barber, 2008; Sun, Li, Chen, Chen, You, Zhou, Zhou, Zhai, Chen and Jiang, 2009; Zhang, Nandakumar, Reinert, Huang, Laustsen, Gao, Sun, Jensen, Troldborg, Assil, Berthelsen, Scavenius, Zhang, Windross, Olagnier, Prabakaran, Bodda, Narita, Cai, Zhang, Stenmark, Doucet, Noda, Guo, Goldbach-Mansky, Hartmann, Chen, Enghild, Bak, Thomsen and Paludan, 2020). Thus, viral targeting of ER retention sequences or the translocation of STING is an evolutionary strategy for viruses to antagonize STING-mediated antiviral immunity. For example, human cytomegalovirus (HCMV) UL82 interacts with STING and impairs STING-mediated signaling by inhibiting STING translocation from the ER to perinuclear microsomes, disrupting the STING-iRhom2-TRAPbeta translocation complex (Fu, et al., 2017); HCMV UL82 also impairs TBK1 and IRF3 recruitment to the STING complex and prevents STING-mediated IRF3 phosphorylation and activation (Fu, Su, Gao, Wang, Huang, Hu, Luo, Li, Luo, Wang and Shu, 2017). HCMV UL94 interacts with STING, disrupts its dimerization and ER translocation, and impairs TBK1 recruitment to the STING signaling pathway (Zou, et al., 2020). HSV-1 gamma134.5 disrupted the translocation of STING from the ER to the Golgi apparatus, inactivating the DNA-sensing pathway and facilitating viral replication (Pan, et al., 2018). In this study, duck STING contains only one ER retention sequence, "R_{82}YRGS$_{86}$," that is conserved with human and mouse STING. This sequence is crucial for DPV US3 to disrupt the association and phosphorylation between STING and TBK1. Additionally, we found that the STING S86A mutant of duck STING attenuated its ability to mediate IFN expression, suggesting that this serine residue may be an important site for host kinase phosphorylation.

Reduction in STING stability and degradation by viruses counteracts STING-mediated antiviral immune responses. As previously reported, human papillomavirus 16 (HPV16) hijacks NLRX1 (NLR family member X1) to promote E7-potentiated STING degradation (Luo, et al., 2020). The E3 ligases, tripartite motif-containing 30 alpha (TRIM30A) and TRIM29, negatively regulate innate immune responses to DNA viruses by targeting STING and promoting its degradation via K48-linked ubiquitination through a proteasome-dependent pathway (Li, et al., 2018; Wang, et al., 2015). African swine fever virus (ASFV) infection promotes ULK1 expression, which phosphorylates and promoting its the degradation of STING via the autophagy pathway (Konno, et al., 2013; Li, et al., 2021). Tyrosine protein phosphatase non-receptor type 1 (PTPN1) and 2 (PTPN2) are associated with STING following viral infection and dephosphorylate STING at Y245, leading to STING degradation via the ubiquitin-independent 20S proteasome pathway, which depends on the intrinsically disordered region (IDR) of STING (Xia, et al., 2019). Notably, duck STING is phosphorylated and degraded by DPV US3 in a kinase activity-dependent manner. Furthermore, we demonstrated that DPV US3 induces STING degradation via the proteasome and autolysosome pathways. The Bcl-2 associated transcription factor 1 (Bclaf1) positively regulates antiviral responses but is degraded by pseudorabies virus (PRV) and herpes simplex virus type 1 (HSV-1), both members of Alphaherpesviridae (Qin, et al., 2019). The protein level of Bclaf1 recovered in US3 virus-infected cells (Qin et al., 2019), indicating that US3 may induce Bclaf1 protein degradation, although the underlying molecular mechanism is unknown. Our study elucidates the mechanism by which the US3 kinase of Alphaherpesviridae induces immune-related adaptor protein degradation and regulates cellular antiviral responses.

Autophagy is also a powerful cell-intrinsic host defense mechanism capable of restricting viral pathogenicity (Choi, et al., 2018). Autophagy is partly regulated by the mechanistic target of rapamycin complex 1 (mTORC1), a multisubunit Ser/Thr kinase that coordinates anabolic and catabolic outputs (Saxton and Sabatini, 2017). While mTORC1 activation stimulates protein synthesis and represses autophagy, the inhibition of mTORC1 by energy, nutrient, or growth factor insufficiency suppresses protein synthesis and promotes autophagy (Saxton and Sabatini, 2017). Inhibition of mTORC1 activates the autophagy regulator ULK1, the Ser/Thr kinase component of the multi-subunit ULK complex, which

induces autophagy by phosphorylating Beclin-1 and activating vacuolar protein sorting 34 (VPS34) lipid kinase (Kim, et al., 2011; Russell, et al., 2013). To counteract autophagy, HSV-1 US3 kinase has been reported to phosphorylate and activate mTORC1 (Vink, et al., 2018), indicating that autophagy initiation is inhibited by US3. Furthermore, the HSV-1 US3 kinase can phosphorylate Beclin-1 and inhibit autophagy (Rubio and Mohr, 2019). In this study, we found that DPV US3 phosphorylates STING, and protein levels of both DPV US3 and STING were reduced when expressed together. STING was recently shown to induce non-canonical antiviral autophagy by interacting with the microtubule-associated protein 1 light chain 3 (LC3B) (Gui, et al., 2019; Liu, et al., 2019). As the degradation of STING and US3 was recovered by inhibiting the proteasome and autolysosome pathways (Fig. 3), we hypothesized that DPV US3 may regulate STING-mediated antiviral autophagy by redirecting STING into another complex for degradation; however, the underlying mechanism requires further investigation.

Conclusion

In summary, our results provide mechanistic insights into how DPV antagonizes host antiviral innate immune responses. We demonstrated that DPV US3 inhibits duck STING-mediated antiviral responses by interacting with and phosphorylating STING at serine 86, near the ER retention sequence. Phosphorylation of STING by DPV US3 kinase reduces STING dimerization, disrupts the interaction between STING and TBK1, reduces STING stability, and induces STING degradation via the proteasome and autolysosome pathways. These findings suggest that DPV US3 kinase modulates duck STING-mediated antiviral responses, thereby promoting DPV replication and pathogenicity.

Disclosures

The authors declare that the research was conducted in the absence of any commerciaor financial relationships that could be construed as a potential conflict of interest.

Declaration of competing interest

The authors declare that they have no known competing financial interests or personal relationships that could have appeared to influence the work reported in this paper.

Acknowledgments

We thank Sichuan Agricultural University for providing the experimental platform and other members of the group for their help. This work was supported by the Program of National Natural Science Foundation of China (NO. 32473042, 32002282), the China Agricultural Research System (NO. CARS-42-17), and the Sichuan Veterinary Medicine and Drug Innovation Group of the China Agricultural Research System (NO. SCCXTD-2020-18).

References

Benetti, L., Roizman, B., 2004. Herpes simplex virus protein kinase US3 activates and functionally overlaps protein kinase A to block apoptosis. Proc. Natl. Acad. Sci. U. S. A. 101, 9411–9416. https://doi.org/10.1073/pnas.0403160101.

Bodda, C., Reinert, L.S., Fruhwurth, S., Richardo, T., Sun, C., Zhang, B.C., Kalamvoki, M., Pohlmann, A., Mogensen, T.H., Bergstrom, P., Agholme, L., O'Hare, P., Sodeik, B., Gyrd-Hansen, M., Zetterberg, H., Paludan, S.R., 2020. HSV1 VP1-2 deubiquitinates STING to block type I interferon expression and promote brain infection. J. Exp. Med. 217. https://doi.org/10.1084/jem.20191422.

Burdette, D.L., Monroe, K.M., Sotelo-Troha, K., Iwig, J.S., Eckert, B., Hyodo, M., Hayakawa, Y., Vance, R.E., 2011. STING is a direct innate immune sensor of cyclic di-GMP. Nature 478, 515–518. https://doi.org/10.1038/nature10429.

Cartier, A., Komai, T., Masucci, M.G., 2003. The Us3 protein kinase of herpes simplex virus 1 blocks apoptosis and induces phosporylation of the Bcl-2 family member Bad. Exp. Cell Res. 291, 242–250. https://doi.org/10.1016/s0014-4827 (03)00375-6.

Chen, Q., Sun, L., Chen, Z.J., 2016. Regulation and function of the cGAS-STING pathway of cytosolic DNA sensing. Nat. Immunol. 17, 1142–1149. https://doi.org/10.1038/ni.3558.

Chen, S., Wu, Z., Zhang, J., Wang, M., Jia, R., Zhu, D., Liu, M., Sun, K., Yang, Q., Wu, Y., Zhao, X., Cheng, A., 2018. Duck stimulator of interferon genes plays an important role in host anti-duck plague virus infection through an IFN-dependent signalling pathway. Cytokine 102, 191–199. https://doi.org/10.1016/j.cyto.2017.09.008.

Chen, S., Zhang, W., Zhou, Q., Wang, A., Sun, L., Wang, M., Jia, R., Zhu, D., Liu, M., Sun, K., Yang, Q., Wu, Y., Chen, X., Cheng, A., 2017. Cross-species antiviral activity of goose interferon lambda against duck plague virus is related to its positive self-regulatory feedback loop. J. Gen. Virol. 98, 1455–1466. https://doi.org/10.1099/jgv.0.000788.

Choi, Y., Bowman, J.W., Jung, J.U., 2018. Autophagy during viral infection - a double-edged sword. Nat. Rev. Microbiol. 16, 341–354. https://doi.org/10.1038/s41579-018-0003-6.

Converse, K.A., Kidd, G.A., 2001. Duck plague epizootics in the United States, 1967-1995. J. Wildl. Dis. 37, 347–357. https://doi.org/10.7589/0090-3558-37.2.347.

Deng, L., Cheng, A., Wang, M., Zhang, W., Tian, B., Wu, Y., Yang, Q., Ou, X., Mao, S., Sun, D., Zhang, S., Huang, J., Gao, Q., Zhao, X., Jia, R., Chen, S., Liu, M., Zhu, D., 2023. Effects of US3 protein kinase activity on localization of UL31/UL34 protein and nucleocapsids egress of duck plague virus. Poult. Sci. 102, 102418. https://doi.org/10.1016/j.psj.2022.102418.

Deng, L., Wan, J., Cheng, A., Wang, M., Tian, B., Wu, Y., Yang, Q., Ou, X., Mao, S., Sun, D., Zhang, S., Zhu, D., Jia, R., Chen, S., Liu, M., Zhao, X., Huang, J., Gao, Q., Yu, Y., Zhang, L., Pan, L., 2022. Duck plague virus US3 protein kinase phosphorylates UL47 and regulates the subcellular localization of UL47. Front. Microbiol. 13, 876820. https://doi.org/10.3389/fmicb.2022.876820.

Deng, L., Wang, M., Cheng, A., Yang, Q., Wu, Y., Jia, R., Chen, S., Zhu, D., Liu, M., Zhao, X., Zhang, S., Huang, J., Ou, X., Mao, S., Zhang, L., Liu, Y., Yu, Y., Tian, B., Pan, L., Rehman, M.U., Chen, X., 2020. The pivotal roles of US3 protein in cell-to-cell spread and virion nuclear egress of duck plague virus. Sci. Rep. 10, 7181. https://doi.org/10.1038/s41598-020-64190-2.

Deschamps, T., Kalamvoki, M., 2017. Evasion of the STING DNA-sensing pathway by VP11/12 of herpes simplex virus 1. J. Virol. 91. https://doi.org/10.1128/JVI.00535-17.

Dhama, K., Kumar, N., Saminathan, M., Tiwari, R., Karthik, K., Kumar, M.A., Palanivelu, M., Shabbir, M.Z., Malik, Y.S., Singh, R.K., 2017. Duck virus enteritis (duck plague) - a comprehensive update. Vet. Q. 37, 57–80. https://doi.org/10.1080/01652176.2017.1298885.

Dobbs, N., Burnaevskiy, N., Chen, D., Gonugunta, V.K., Alto, N.M., Yan, N., 2015. STING activation by translocation from the ER Is associated with infection and autoinflammatory disease. Cell Host Microbe 18, 157–168. https://doi.org/10.1016/j.chom.2015.07.001.

Fu, Y.Z., Su, S., Gao, Y.Q., Wang, P.P., Huang, Z.F., Hu, M.M., Luo, W.W., Li, S., Luo, M. H., Wang, Y.Y., Shu, H.B., 2017. Human cytomegalovirus tegument protein UL82 inhibits STING-mediated signaling to evade antiviral immunity. Cell Host Microbe 21, 231–243. https://doi.org/10.1016/j.chom.2017.01.001.

Gao, P., Ascano, M., Zillinger, T., Wang, W., Dai, P., Serganov, A.A., Gaffney, B.L., Shuman, S., Jones, R.A., Deng, L., Hartmann, G., Barchet, W., Tuschl, T., Patel, D.J., 2013. Structure-function analysis of STING activation by c[G (2′,5′)pA (3′,5′)p] and targeting by antiviral DMXAA. Cell 154, 748–762. https://doi.org/10.1016/j.cell.2013.07.023.

Gui, X., Yang, H., Li, T., Tan, X., Shi, P., Li, M., Du, F., Chen, Z.J., 2019. Autophagy induction via STING trafficking is a primordial function of the cGAS pathway. Nature 567, 262–266. https://doi.org/10.1038/s41586-019-1006-9.

Huang, J., You, H., Su, C., Li, Y., Chen, S., Zheng, C., 2018. Herpes simplex virus 1 tegument protein VP22 abrogates cGAS/STING-mediated antiviral innate immunity. J. Virol. 92. https://doi.org/10.1128/JVI.00841-18.

Ishikawa, H., Barber, G.N., 2008. STING is an endoplasmic reticulum adaptor that facilitates innate immune signalling. Nature 455, 674–678. https://doi.org/10.1038/nature07317.

Ishikawa, H., Barber, G.N., 2011. The STING pathway and regulation of innate immune signaling in response to DNA pathogens. Cell Mol. Life Sci. 68, 1157–1165. https://doi.org/10.1007/s00018-010-0605-2.

Jansens, R.J.J., Van den Broeck, W., De Pelsmaeker, S., Lamote, J.A.S., Van Waesberghe, C., Couck, L., Favoreel, H.W., 2017. Pseudorabies virus US3-induced tunneling nanotubes contain stabilized microtubules, interact with neighboring cells via cadherins, and allow intercellular molecular communication. J. Virol. 91. https://doi.org/10.1128/JVI.00749-17.

Jung, M., Finnen, R.L., Neron, C.E., Banfield, B.W., 2011. The alphaherpesvirus serine/threonine kinase us3 disrupts promyelocytic leukemia protein nuclear bodies. J. Virol. 85, 5301–5311. https://doi.org/10.1128/JVI.00022-11.

Kato, A., Shindo, K., Maruzuru, Y., Kawaguchi, Y., 2014. Phosphorylation of a herpes simplex virus 1 dUTPase by a viral protein kinase, Us3, dictates viral pathogenicity in the central nervous system but not at the periphery. J. Virol. 88, 2775–2785. https://doi.org/10.1128/JVI.03300-13.

Kim, J., Kundu, M., Viollet, B., Guan, K.L., 2011. AMPK and mTOR regulate autophagy through direct phosphorylation of Ulk1. Nat. Cell Biol. 13, 132–141. https://doi.org/10.1038/ncb2152.

Konno, H., Konno, K., Barber, G.N., 2013. Cyclic dinucleotides trigger ULK1 (ATG1) phosphorylation of STING to prevent sustained innate immune signaling. Cell 155, 688–698. https://doi.org/10.1016/j.cell.2013.09.049.

Leader, D.P., 1993. Viral protein kinases and protein phosphatases. Pharmacol. Ther. 59, 343–389. https://doi.org/10.1016/0163-7258 (93)90075-o.

Leader, D.P., Deana, A.D., Marchiori, F., Purves, F.C., Pinna, L.A., 1991. Further definition of the substrate specificity of the alpha-herpesvirus protein kinase and

comparison with protein kinases A and C. Biochim. Biophys. Acta 1091, 426–431. https://doi.org/10.1016/0167-4889 (91)90210-o.
Li, D., Yang, W., Li, L., Li, P., Ma, Z., Zhang, J., Qi, X., Ren, J., Ru, Y., Niu, Q., Liu, Z., Liu, X., Zheng, H., 2021. African swine fever virus MGF-505-7R negatively regulates cGAS-STING-mediated signaling pathway. J. Immunol. 206, 1844–1857. https://doi.org/10.4049/jimmunol.2001110.
Li, D., Yang, W., Ren, J., Ru, Y., Zhang, K., Fu, S., Liu, X., Zheng, H., 2019. The E3 ubiquitin ligase TBK1 mediates the degradation of multiple picornavirus VP3 proteins by phosphorylation and ubiquitination. J. Virol. 93. https://doi.org/10.1128/jvi.01438-19.
Li, N., Hong, T., Li, R., Guo, M., Wang, Y., Zhang, J., Liu, J., Cai, Y., Liu, S., Chai, T., Wei, L., 2016. Pathogenicity of duck plague and innate immune responses of the Cherry Valley ducks to duck plague virus. Sci. Rep. 6, 32183. https://doi.org/10.1038/srep32183.
Li, Q., Lin, L., Tong, Y., Liu, Y., Mou, J., Wang, X., Wang, X., Gong, Y., Zhao, Y., Liu, Y., Zhong, B., Dai, L., Wei, Y.Q., Zhang, H., Hu, H., 2018. TRIM29 negatively controls antiviral immune response through targeting STING for degradation. Cell Discov. 4, 13. https://doi.org/10.1038/s41421-018-0010-9.
Liu, D., Wu, H., Wang, C., Li, Y., Tian, H., Siraj, S., Sehgal, S.A., Wang, X., Wang, J., Shang, Y., Jiang, Z., Liu, L., Chen, Q., 2019. STING directly activates autophagy to tune the innate immune response. Cell Death Differ. 26, 1735–1749. https://doi.org/10.1038/s41418-018-0251-z.
Liu, R., Gao, L., Yang, F., Li, X., Liu, C., Qi, X., Cui, H., Zhang, Y., Wang, S., Wang, X., Gao, Y., Li, K., 2022a. Duck enteritis virus protein kinase US3 inhibits DNA sensing signaling by phosphorylating interferon regulatory factor 7. Microbiol. Spectr., e0229922 https://doi.org/10.1128/spectrum.02299-22.
Liu, R., Gao, L., Yang, F., Li, X., Liu, C., Qi, X., Cui, H., Zhang, Y., Wang, S., Wang, X., Gao, Y., Li, K., 2022b. Duck enteritis virus protein kinase US3 inhibits DNA sensing signaling by phosphorylating interferon regulatory factor 7. Microbiol. Spectr. 10, e0229922. https://doi.org/10.1128/spectrum.02299-22.
Liu, S., Cai, X., Wu, J., Cong, Q., Chen, X., Li, T., Du, F., Ren, J., Wu, Y.T., Grishin, N.V., Chen, Z.J., 2015. Phosphorylation of innate immune adaptor proteins MAVS, STING, and TRIF induces IRF3 activation. Science 347, aaa2630. https://doi.org/10.1126/science.aaa2630, 1979).
Luo, X., Donnelly, C.R., Gong, W., Heath, B.R., Hao, Y., Donnelly, L.A., Moghbeli, T., Tan, Y.S., Lin, X., Bellile, E., Kansy, B.A., Carey, T.E., Brenner, J.C., Cheng, L., Polverini, P.J., Morgan, M.A., Wen, H., Prince, M.E., Ferris, R.L., Xie, Y., Young, S., Wolf, G.T., Chen, Q., Lei, Y.L., 2020. HPV16 drives cancer immune escape via NLRX1-mediated degradation of STING. J. Clin. Invest. 130, 1635–1652. https://doi.org/10.1172/JCI129497.
Ma, Z., Bai, J., Jiang, C., Zhu, H., Liu, D., Pan, M., Wang, X., Pi, J., Jiang, P., Liu, X., 2023. Tegument protein UL21 of alpha-herpesvirus inhibits the innate immunity by triggering CGAS degradation through TOLLIP-mediated selective autophagy. Autophagy 19, 1512–1532. https://doi.org/10.1080/15548627.2022.2139921.
Ogg, P.D., McDonell, P.J., Ryckman, B.J., Knudson, C.M., Roller, R.J., 2004. The HSV-1 Us3 protein kinase is sufficient to block apoptosis induced by overexpression of a variety of Bcl-2 family members. Virology 319, 212–224. https://doi.org/10.1016/j.virol.2003.10.019.
Pan, S., Liu, X., Ma, Y., Cao, Y., He, B., 2018. Herpes simplex virus 1 gamma134.5 protein inhibits STING activation that restricts viral replication. J. Virol. 92. https://doi.org/10.1128/JVI.01015-18.
Purves, F.C., Deana, A.D., Marchiori, F., Leader, D.P., Pinna, L.A., 1986. The substrate specificity of the protein kinase induced in cells infected with herpesviruses: studies with synthetic substrates [corrected] indicate structural requirements distinct from other protein kinases. Biochim. Biophys. Acta 889, 208–215. https://doi.org/10.1016/0167-4889 (86)90106-0.
Qi, X., Yang, X., Cheng, A., Wang, M., Guo, Y., Jia, R., 2009. Replication kinetics of duck virus enteritis vaccine virus in ducklings immunized by the mucosal or systemic route using real-time quantitative PCR. Res. Vet. Sci. 86, 63–67. https://doi.org/10.1016/j.rvsc.2008.05.001.
Qi, X., Yang, X., Cheng, A., Wang, M., Zhu, D., Jia, R., 2008. Quantitative analysis of virulent duck enteritis virus loads in experimentally infected ducklings. Avian Dis. 52, 338–344. https://doi.org/10.1637/8120-100207-ResNote.1.
Qin, C., Zhang, R., Lang, Y., Shao, A., Xu, A., Feng, W., Han, J., Wang, M., He, W., Yu, C., Tang, J., 2019. Bclaf1 critically regulates the type I interferon response and is degraded by alphaherpesvirus US3. PLoS Pathog. 15, e1007559. https://doi.org/10.1371/journal.ppat.1007559.
Rao, P., Pham, H.T., Kulkarni, A., Yang, Y., Liu, X., Knipe, D.M., Cresswell, P., Yuan, W., 2011. Herpes simplex virus 1 glycoprotein B and US3 collaborate to inhibit CD1d antigen presentation and NKT cell function. J. Virol. 85, 8093–8104. https://doi.org/10.1128/JVI.02689-10.
Roizmann, B., Desrosiers, R.C., Fleckenstein, B., Lopez, C., Minson, A.C., Studdert, M.J., 1992. The family herpesviridae: an update. the herpesvirus study group of the international committee on taxonomy of viruses. Arch. Virol. 123, 425–449. https://doi.org/10.1007/BF01317276.
Rubio, R.M., Mohr, I., 2019. Inhibition of ULK1 and Beclin1 by an alpha-herpesvirus Akt-like Ser/Thr kinase limits autophagy to stimulate virus replication. Proc. Natl. Acad. Sci. U. S. A. https://doi.org/10.1073/pnas.1915139116.
Russell, R.C., Tian, Y., Yuan, H., Park, H.W., Chang, Y.Y., Kim, J., Kim, H., Neufeld, T.P., Dillin, A., Guan, K.L., 2013. ULK1 induces autophagy by phosphorylating Beclin-1 and activating VPS34 lipid kinase. Nat. Cell Biol. 15, 741–750. https://doi.org/10.1038/ncb2757.
Saxton, R.A., Sabatini, D.M., 2017. mTOR signaling in growth, metabolism, and disease. Cell 169, 361–371. https://doi.org/10.1016/j.cell.2017.03.035.
Sun, W., Li, Y., Chen, L., Chen, H., You, F., Zhou, X., Zhou, Y., Zhai, Z., Chen, D., Jiang, Z., 2009. ERIS, an endoplasmic reticulum IFN stimulator, activates innate immune signaling through dimerization. Proc. Natl. Acad. Sci. U. S. A. 106, 8653–8658. https://doi.org/10.1073/pnas.0900850106.
Tanaka, Y., Chen, Z.J., 2012. STING specifies IRF3 phosphorylation by TBK1 in the cytosolic DNA signaling pathway. Sci. Signal. 5. https://doi.org/10.1126/scisignal.2002521 ra20.
Tian, B., Cai, D., He, T., Deng, L., Wu, L., Wang, M., Jia, R., Zhu, D., Liu, M., Yang, Q., Wu, Y., Zhao, X., Chen, S., Zhang, S., Huang, J., Ou, X., Mao, S., Yu, Y., Zhang, L., Liu, Y., Cheng, A., 2019. Isolation and selection of duck primary cells as pathogenic and innate immunologic cell models for duck plague virus. Front. Immunol. 10, 3131. https://doi.org/10.3389/fimmu.2019.03131.
Tian, J., Liu, Y., Liu, X., Sun, X., Zhang, J., Qu, L., 2018. Feline Herpesvirus 1 US3 blocks the type i interferon signal pathway by targeting interferon regulatory factor 3 dimerization in a kinase-independent manner. J. Virol. 92. https://doi.org/10.1128/JVI.00047-18.
Tian, Y., Tian, B., Wang, M., Cai, D., Cheng, A., Zhang, W., Wu, Y., Yang, Q., Ou, X., Sun, D., Zhang, S., Mao, S., Zhao, X., Huang, J., Gao, Q., Zhu, D., Jia, R., Chen, S., Liu, M., 2023. BX795, a kinase inhibitor, inhibit duck plague virus infection via targeting US3 kinase. Poult. Sci. 102, 102597. https://doi.org/10.1016/j.psj.2023.102597.
Vink, E.I., Lee, S., Smiley, J.R., Mohr, I., 2018. Remodeling mTORC1 responsiveness to amino acids by the herpes simplex virus UL46 and Us3 Gene Products Supports Replication during Nutrient Insufficiency. J. Virol. 92. https://doi.org/10.1128/JVI.01377-18.
Wang, K., Ni, L., Wang, S., Zheng, C., 2014. Herpes simplex virus 1 protein kinase US3 hyperphosphorylates p65/RelA and dampens NF-kappaB activation. J. Virol. 88, 7941–7951. https://doi.org/10.1128/JVI.03394-13.
Wang, S., Wang, K., Lin, R., Zheng, C., 2013. Herpes simplex virus 1 serine/threonine kinase US3 hyperphosphorylates IRF3 and inhibits beta interferon production. J. Virol. 87, 12814–12827. https://doi.org/10.1128/JVI.02355-13.
Wang, X., Patenode, C., Roizman, B., 2011. US3 protein kinase of HSV-1 cycles between the cytoplasm and nucleus and interacts with programmed cell death protein 4 (PDCD4) to block apoptosis. Proc. Natl. Acad. Sci. U. S. A. 108, 14632–14636. https://doi.org/10.1073/pnas.1111942108.
Wang, Y., Lian, Q., Yang, B., Yan, S., Zhou, H., He, L., Lin, G., Lian, Z., Jiang, Z., Sun, B., 2015. TRIM30alpha is a negative-feedback regulator of the intracellular DNA and DNA virus-triggered response by targeting STING. PLoS Pathog. 11, e1005012. https://doi.org/10.1371/journal.ppat.1005012.
Wu, J., Sun, L., Chen, X., Du, F., Shi, H., Chen, C., Chen, Z.J., 2013. Cyclic GMP-AMP is an endogenous second messenger in innate immune signaling by cytosolic DNA. Science 339, 826–830. https://doi.org/10.1126/science.1229963, 1979).
Xia, T., Yi, X.M., Wu, X., Shang, J., Shu, H.B., 2019. PTPN1/2-mediated dephosphorylation of MITA/STING promotes its 20S proteasomal degradation and attenuates innate antiviral response. Proc. Natl. Acad. Sci. U. S. A. 116, 20063–20069. https://doi.org/10.1073/pnas.1906431116.
Xiong, R., Rao, P., Kim, S., Li, M., Wen, X., Yuan, W., 2015. Herpes simplex virus 1 US3 phosphorylates cellular KIF3A To downregulate CD1d expression. J. Virol. 89, 6646–6655. https://doi.org/10.1128/JVI.00214-15.
Xu, H., Su, C., Pearson, A., Mody, C.H., Zheng, C., 2017. Herpes simplex virus 1 UL24 abrogates the DNA sensing signal pathway by inhibiting NF-kappaB activation. J. Virol. 91. https://doi.org/10.1128/JVI.00025-17.
You, H., Lin, Y., Lin, F., Yang, M., Li, J., Zhang, R., Huang, Z., Shen, Q., Tang, R., Zheng, C., 2020. beta-catenin is required for the cGAS/STING signaling pathway but antagonized by the herpes simplex virus 1 US3 protein. J. Virol. 94. https://doi.org/10.1128/JVI.01847-19.
You, H., Zheng, S., Huang, Z., Lin, Y., Shen, Q., Zheng, C., 2019. Herpes simplex virus 1 tegument protein UL46 inhibits TANK-binding kinase 1-mediated signaling. mBio 10. https://doi.org/10.1128/mBio.00919-19.
You, Y., Cheng, A.C., Wang, M.S., Jia, R.Y., Sun, K.F., Yang, Q., Wu, Y., Zhu, D., Chen, S., Liu, M.F., Zhao, X.X., Chen, X.Y., 2017. The suppression of apoptosis by alpha-herpesvirus. Cell Death Dis. 8, e2749. https://doi.org/10.1038/cddis.2017.139.
Yuan, G.P., Cheng, A.C., Wang, M.S., Liu, F., Han, X.Y., Liao, Y.H., Xu, C., 2005. Electron microscopic studies of the morphogenesis of duck enteritis virus. Avian Dis. 49, 50–55. https://doi.org/10.1637/7237-071004R.
Zhang, B.C., Nandakumar, R., Reinert, L.S., Huang, J., Laustsen, A., Gao, Z.L., Sun, C.L., Jensen, S.B., Troldborg, A., Assil, S., Berthelsen, M.F., Scavenius, C., Zhang, Y., Windross, S.J., Olagnier, D., Prabakaran, T., Bodda, C., Narita, R., Cai, Y., Zhang, C. G., Stenmark, H., Doucet, C.M., Noda, T., Guo, Z., Goldbach-Mansky, R., Hartmann, R., Chen, Z.J., Enghild, J.J., Bak, R.O., Thomsen, M.K., Paludan, S.R., 2020. STEEP mediates STING ER exit and activation of signaling. Nat. Immunol. 21, 868–879. https://doi.org/10.1038/s41590-020-0730-5.
Zhang, K., Donovan, T., Sucharita, S., Brownlie, R., Snider, M., Tikoo, S.K., van Drunen Littel-van den Hurk, S., 2019. US3 kinase-mediated phosphorylation of tegument protein VP8 Plays a critical role in the cellular localization of VP8 and its effect on the lipid metabolism of bovine herpesvirus 1-infected cells. J. Virol. 93. https://doi.org/10.1128/JVI.02151-18.
Zhao, B., Du, F., Xu, P., Shu, C., Sankaran, B., Bell, S.L., Liu, M., Lei, Y., Gao, X., Fu, X., Zhu, F., Liu, Y., Laganowsky, A., Zheng, X., Ji, J.Y., West, A.P., Watson, R.O., Li, P., 2019. A conserved PLPLRT/SD motif of STING mediates the recruitment and

activation of TBK1. Nature 569, 718–722. https://doi.org/10.1038/s41586-019-1228-x.

Zhong, B., Yang, Y., Li, S., Wang, Y.Y., Li, Y., Diao, F., Lei, C., He, X., Zhang, L., Tien, P., Shu, H.B., 2008. The adaptor protein MITA links virus-sensing receptors to IRF3 transcription factor activation. Immunity 29, 538–550. https://doi.org/10.1016/j.immuni.2008.09.003.

Zou, H.M., Huang, Z.F., Yang, Y., Luo, W.W., Wang, S.Y., Luo, M.H., Fu, Y.Z., Wang, Y.Y., 2020. Human cytomegalovirus protein UL94 targets MITA to evade the antiviral immune response. J. Virol. 94. https://doi.org/10.1128/JVI.00022-20.